Aluminum Complexes as Models for Broensted Acid Sites in Zeolites: Structure and Energetics of $[Al(OH)_4]^-$, $[Al(H_2O)_6]^{3+}$, and Intermediate Monomeric Species $[Al(OH)_x(H_2O)_{n-x}{\cdot}mH_2O]^{3-x}$ Obtained by Hydrolysis

James M. Ruiz,*,† Mark H. McAdon, and Juan M. Garcés

The Dow Chemical Company, Central & New Businesses Research and Development, 1776 Building, Midland, Michigan 48674

Received: July 3, 1996; In Final Form: December 9, 1996[⊗]

Using ab initio quantum mechanical methods, we examined cluster models for the transformation of aluminum sites in zeolites from tetrahedral to octahedral coordination. We investigated the relative stability of tetracoordinated, pentacoordinated, and hexacoordinated aluminum at different degrees of ligand protonation using monomeric aluminum hydroxy−aquo complexes of the form $[Al(OH)_x(H_2O)_{n-x}]^{3-x}$. For $n = 4$ and $n = 5$, we also investigated complexes having water in the second coordination sphere, i.e., $[Al(OH)_x(H_2O)_{n-x}{\cdot}mH_2O]^{3-x}$, $n + m = 6$. A shift in preference from tetra- to hexacoordination occurred when the net charge on a complex was equal to or greater than +1. Hydrogen bonds were found to be very important in stabilizing the pentacoordinated and hexacoordinated species, especially for the highly protonated complexes. Trends in bond lengths, angles, and ligand orientations were identified as functions of coordination number and complex charge.

Introduction

Zeolites are high surface area microporous crystalline aluminosilicates containing 3−15 Å diameter cavities and channels that restrict the motions of guest molecules, such as water, cations, hydrocarbons, etc. Zeolite molecular sieves are used in a variety of applications, including ion exchange, water conditioning and purification, and catalysis, where high selectivities are attainable because of space constraints and diffusional control. Zeolite properties are highly dependent on the Si/Al ratio, since each aluminum carries a negative charge that must be neutralized by a cation, such as $[H]^+$ or $[Na]^+$ in for example $[Na_xAl_xSi_{1-x}O_2]$. The Si/Al ratio depends on the details of the zeolite synthesis and on post-synthetic treatments. The Si/Al ratio can be modified by treatment with acids or bases in combination with heat treatments.

In the design of zeolites for catalytic applications, careful control of Broensted and Lewis acid sites is required, to both tailor activity and prevent deactivation by pore plugging or decomposition. Here, it is assumed that the tetrahedrally coordinated aluminum within the framework is transformed to octahedral species outside of the framework. This transformation is not well understood. It is normally assumed that all framework aluminum is tetrahedrally coordinated, i.e., that octahedrally coordinated aluminum cannot exist within the framework. However, recent evidence for zeolites H−rho[1] and mordenite[2] suggests that octahedral Al species can also exist within the framework.

Since the transformation from tetrahedral to octahedral aluminum is difficult to examine experimentally, we investigated this transformation using computational molecular orbital theory (quantum mechanics), where we used aluminum complexes and clusters as the simplest models for aluminum sites in zeolites. In these complexes, Al−OSi zeolite fragments are approximated by Al−OH fragments. Although the hydrogen for silicon approximation will affect the geometries and energies of aluminum complexes, the effects should be second order in how they affect the aluminum. Therefore, the trends found below for the change in aluminum coordination would not be expected to alter significantly.

We carried out a comprehensive search for stable, monomeric aluminum hydroxy−aquo complexes having coordination numbers $n = 4$, 5, and 6, i.e., $[Al(OH)_x(H_2O)_{n-x}]^{3-x}$. For $n = 4$ and $n = 5$, we also investigated complexes having water in the second coordination sphere, i.e., $[Al(OH)_x(H_2O)_{n-x}{\cdot}mH_2O]^{3-x}$, $n + m = 6$. Optimized geometries and relative energies are reported for each of these complexes. Structural and energetic trends as a function of the coordination number and protonation level were identified. The factors contributing to the formation of octahedral aluminum complexes were determined. These results can be used in the interpretation of current and future experiments and also in the construction of models for extended zeolite frameworks. They also serve as a stepping stone toward understanding the fundamentals of acidity in oxides containing metals in different coordinations.

Background

Understanding the chemistry of aluminum hydroxy−aquo complexes is useful in understanding aluminum in zeolites. Here we provide only a brief review; additional details are given elsewhere.[3,4]

The hexaaquo complex, $Al(H_2O)_6^{3+}$, is well-known and stable both in solution (pH < 5) and in alum salts such as $[NaAl(SO_4)_2{\cdot}12H_2O]$. At high pH and low concentration, the stable species is $[Al(OH)_4]^-$. At intermediate pH levels, the stable species are presumably oligomeric complexes with bridging hydroxyl groups, such as $[Al_2(\mu\text{-}OH)_2(H_2O)_8]^{4+}$, $[AlO_4Al_{12}(OH)_{24}(H_2O)_{12}]^{7+}$, and $[Al_3(OH)_{11}]^{2-}$. Five-coordinate aluminum hydroxy−aquo species are unknown. The identities of these intermediate species are highly dependent on the conditions, such as pH, and concentrations of aluminum, sodium, chloride, carbonate, etc. Hence, structural data are difficult to obtain from experiments. Calculations are useful in this regard, because the structures and energetics of hypothetical structures can be analyzed.

† Current address: Dow Chemical Co., 2301 N. Brazosport Blvd. B-1470, Freeport, TX 77541.

⊗ Abstract published in *Advance ACS Abstracts,* February 1, 1997.

S1089-5647(96)01987-6 CCC: $14.00

Procedure

Molecular orbital (MO) calculations were carried out for aluminum complexes $[Al(OH)_x(H_2O)_{n-x}]^{3-x}$ having coordination numbers $n = 4$, 5, and 6. For $n = 4$ and $n = 5$, complexes having water in the second coordination sphere were also investigated, i.e., $[Al(OH)_x(H_2O)_{n-x}\cdot mH_2O]^{3-x}$, $n + m = 6$.

Our strategy entailed comparing the energies of complexes with the same atomic composition (i.e., isomers). For example, to compare the energies of the hexacoordinated complex $[Al(OH)(H_2O)_5]^{2+}$ with complexes of lower coordination, water molecules were added to the second coordination shells of the penta- and tetracoordination complexes to become $[Al(OH)(H_2O)_4\cdot H_2O]^{2+}$ and $[Al(OH)(H_2O)_3\cdot 2H_2O]^{2+}$. Hence, this strategy also includes the energy component of complex association

$$[Al(OH)_x(H_2O)_{n-x}]^{3-x} + H_2O \rightarrow [Al(OH)_x(H_2O)_{n-x}\cdot H_2O]^{3-x}$$

which is exothermic by 10−30 kcal/mol.[5−7]

Relatively high quality computational methods were used because the energy differences between different isomers can be small (ca. 5 kcal/mol or less). Structures and total energies for the various complexes were calculated using a standard method of electronic structure theory, HF/6-31G* (Hartree−Fock). The Hartree−Fock method is a rigorous ab initio method and contains no adjustable parameters. Basis sets of this type previously gave accurate geometries for similar Si and Al complexes.[9−14] The 6-31G* basis set is a split-valence polarized basis set and is superior to other basis sets such as 3-21G(*) or STO-3G.[8] Earlier HF/3-21G(*) calculations carried out by us were found to overestimate hydrogen-bonding effects and hence were abandoned.

The 6-31G* nomenclature indicates that atomic orbitals in the valence shell are described by two basis functions: one a linear combination of three Gaussian primitive functions and the other a single Gaussian primitive function. Nonvalence atomic orbitals are constructed from six Gaussian primitive functions. So for example in the case of oxygen, the 1s atomic orbital is described by one basis function of six Gaussian primitive functions, and the 2s and 2p orbitals are each described by two basis functions of three and one Gaussian primitive functions, respectively. The * nomenclature indicates that, in addition to the basis functions already described, a set of higher angular momentum basis functions is added for each atom. In the case of oxygen, a set of d basis functions is added to the basis set. In general, as more functions are included in the basis set, the better are the calculated molecular properties.

In all cases, the reported structures were optimized by minimizing the HF/6-31G* total energy with respect to all degrees of freedom, e.g., bond lengths, bond angles, and dihedral angles. Structures were optimized using the standard iterative gradient methods using one of two programs: SPARTAN[15] or GAUSSIAN 92.[16] As expected, these two programs gave nearly identical results. HF/6-31G* optimizations were initially carried out without symmetry constraints, but symmetry was included later only if the final geometries were approaching a symmetrical stationary point. Initial structures were constructed and coarsely optimized using several different methods within the SPARTAN electronic structure program: molecular mechanics, the AM1 semiempirical MO method,[17] or HF/3-21G(*). HF/6-31G* atomic charges were calculated using the electrostatic potential method of SPARTAN.[15]

Our goal was to generate the lowest energy structure of each composition and coordination number (isomer type). For complexes with waters in the second coordination sphere, different orientations can lead to similar energies. In these cases, we investigated several, but not all possible, orientations. We imposed several conditions on the orientations of these second-shell waters in order to ensure that they were reasonable models for aluminum sites embedded in zeolite frameworks. These conditions are given in section IVB. For some cases we may not have found the lowest energy structure, but we believe that our lowest energy structures have total energies no more than 0.5 kcal/mol higher than any structures we may have missed or any structures not allowed by the conditions that we imposed. Hence, the main results of this paper should not be affected by the lack of complete conformational searching or by the imposed conditions.

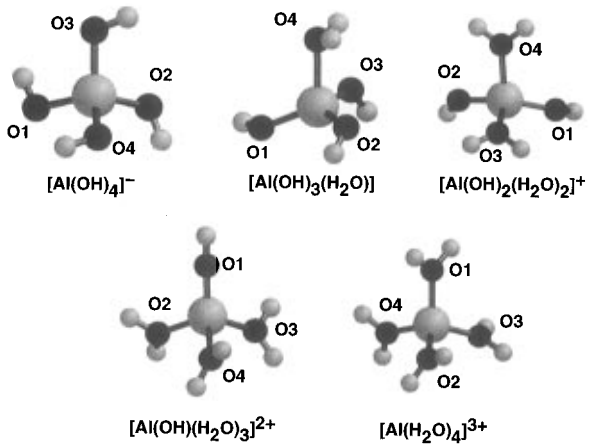

Figure 1. HF/6-31G* optimized structures for naked tetrahedral aluminum aquo−hydroxy complexes. Structural parameters, including bond lengths, bond angles, and dihedral angles, are given in Supporting Information.

For several complexes where the energy differences at the HF/6-31G* level of theory were small, energies were calculated using the Møller−Plesset perturbation theory method (second order; MP2).[18] These "single-point" MP2 energy calculations were carried out for structures optimized at the HF/6-31G* level of theory. The standard notation for such calculations is MP2/6-31G*//HF/6-31G*. The MP2 method includes corrections to the molecular orbital approximation due to electron correlation effects.[19a] In each case, the HF and MP2 relative energetics were similar; hence, it was unnecessary to go to higher levels of theory, such as MP4 (fourth-order perturbation theory). The MP2 energetics are presumed to be superior to the HF energetics.

Results

Results are first presented for the "naked" complexes for coordination numbers $n = 4$, 5, and 6, i.e., the $[Al(OH)_x(H_2O)_{n-x}]^{3-x}$ complexes without water molecules in the second coordination sphere (see Figures 1−3). Structural trends are given in Figures 4−8. Additional details are given in the Supporting Information, including comprehensive tabulations of bond lengths, bond angles, atomic coordinates, and atomic charges. Next, results are presented for complexes having one or two water molecules in the second coordination sphere, as shown in Figures 9 for $[Al(OH)_x(H_2O)_{4-x}\cdot 2H_2O]^{3-x}$ and in Figure 10 for $[Al(OH)_x(H_2O)_{5-x}\cdot H_2O]^{3-x}$. Structural trends for these complexes are given in Figures 11−16, with additional details given in the Supporting Information. We then examine the energetics involved in transformations from tetrahedral coordination to pentacoordinated and octahedral coordinations as the level of protonation is increased.

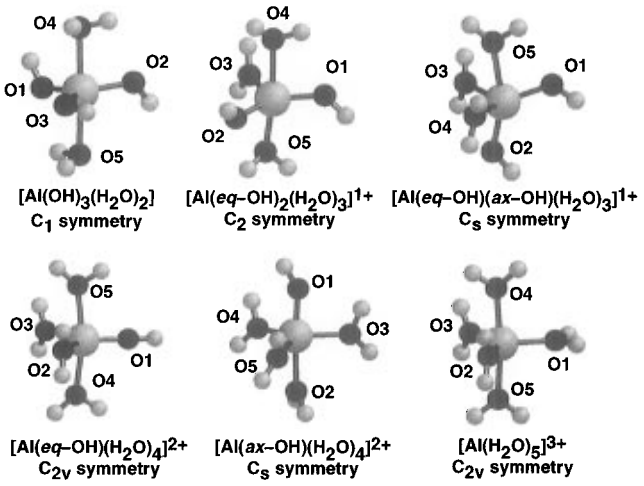

Figure 2. HF/6-31G* optimized structures for naked pentacoordinated aluminum aquo−hydroxy complexes. Structural parameters, including bond lengths and bond angles, are given in Supporting Information.

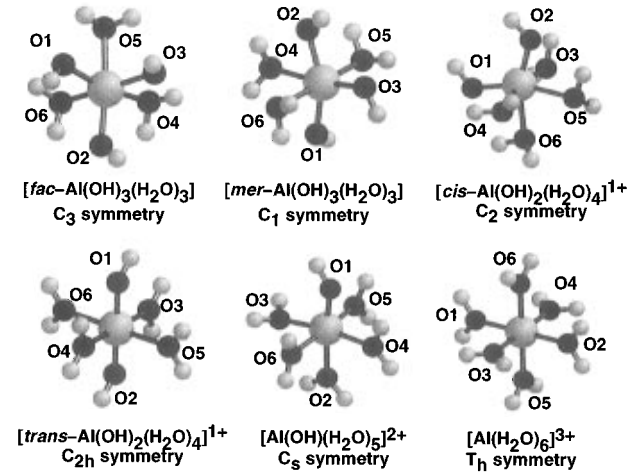

Figure 3. HF/6-31G* optimized structures for naked octahedral aluminum aquo−hydroxy complexes. Structural parameters, including bond lengths and bond angles, are given in Supporting Information.

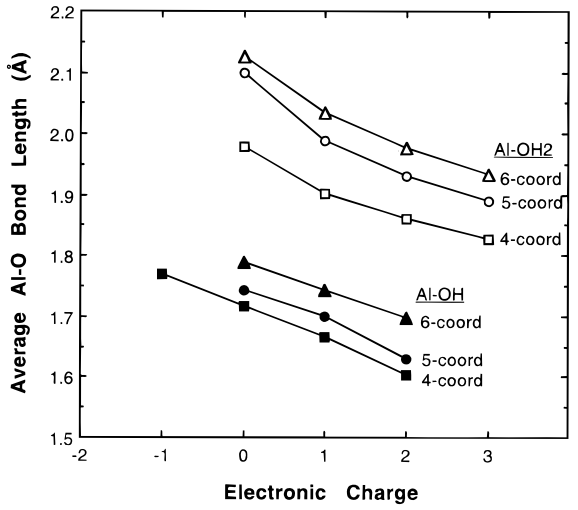

Figure 4. Average Al−O bond length as a function of the degree of protonation for Al−OH and Al−OH_2, from HF/6-31G* structure optimizations. Trends are shown for coordination numbers $n = 4$, 5, and 6.

A. Naked Complexes. The HF/6-31G* calculated energies for the naked complexes are given in Table 1. Figures 1−3 show the structures of these complexes. For fixed coordination number, the various aluminum complexes $[Al(OH)_x(H_2O)_{n-x}]^{3-x}$ exhibit certain structural trends as a function of the degree of protonation, as measured by the net electronic charge of the complex q (where $q = 3 - x$, e.g., $q = -1$ for the $[Al(OH)_4]^-$ complex). These trends are shown in Figures 4−6, which

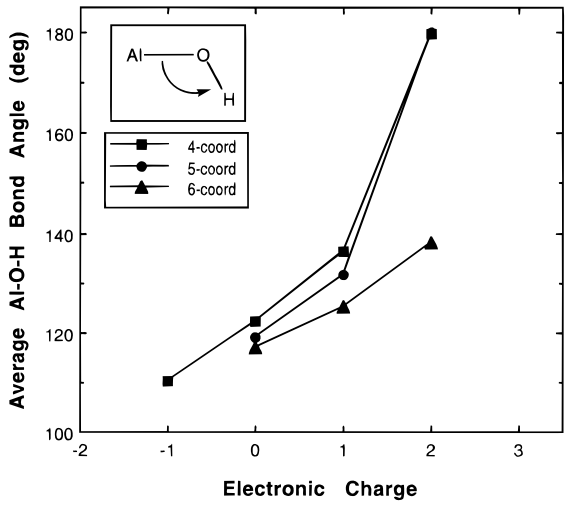

Figure 5. Average Al−O−H bond angle as a function of the protonation level for −OH ligands and coordination numbers $n = 4$, 5, and 6.

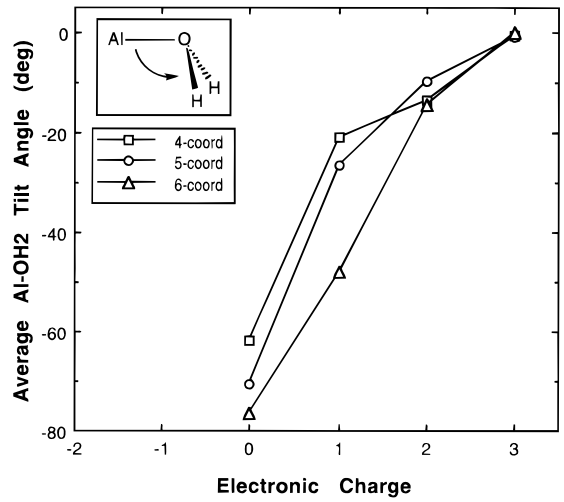

Figure 6. Average Al−OH_2 tilt angle as a function of the protonation level for coordination numbers $n = 4$, 5, and 6.

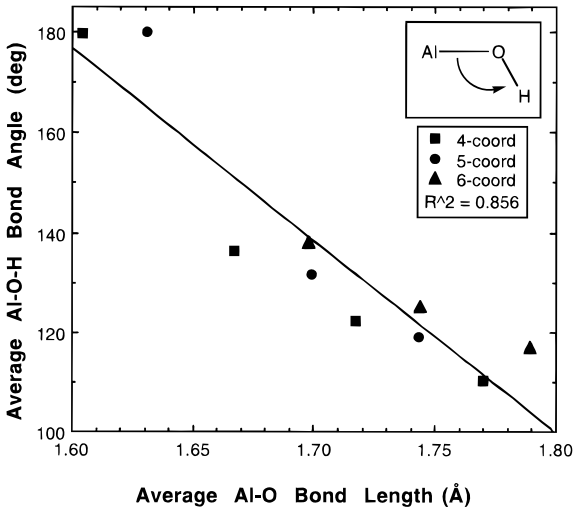

Figure 7. Correlation between the average Al−O−H bond angle and the average Al−O bond length for −OH ligands and coordination numbers $n = 4$, 5, and 6.

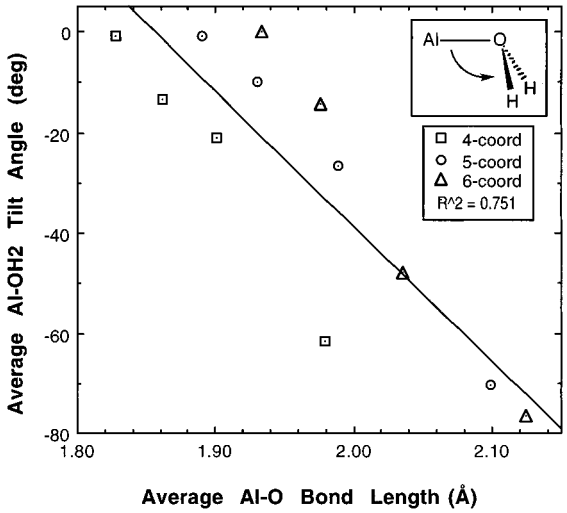

Figure 8. Correlation between the average Al−OH_2 tilt angle and the average Al−O bond length for coordination numbers $n = 4$, 5, and 6.

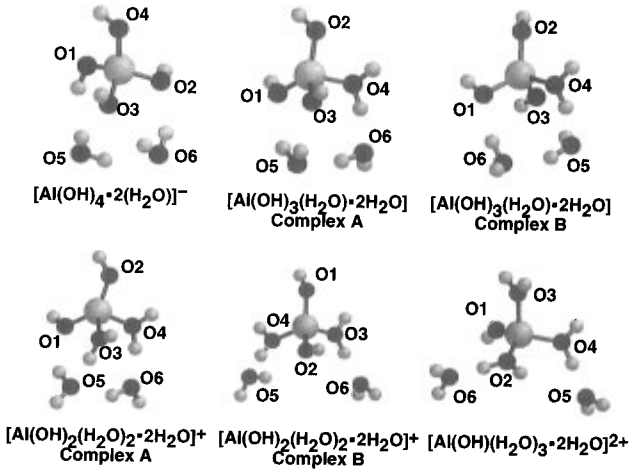

Figure 9. HF/6-31G* optimized structures for tetrahedral aluminum aquo−hydroxy complexes containing two second-shell water molecules. Structural parameters, including bond lengths and bond angles, are given in Supporting Information.

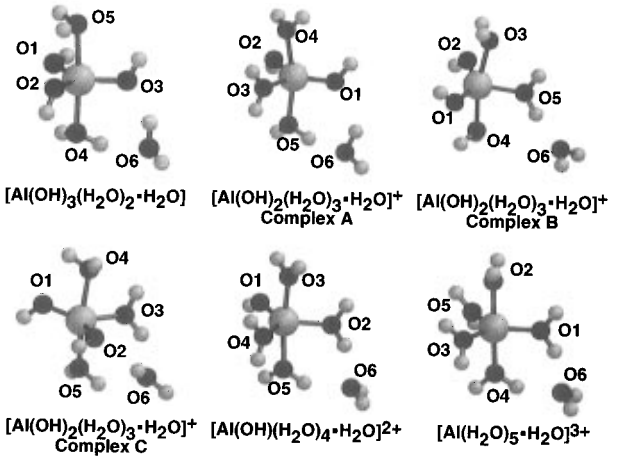

Figure 10. HF/6-31G* optimized structures for pentacoordinated aluminum aquo−hydroxy complexes containing one second-shell water molecule. Structural parameters, including bond lengths and bond angles, are given in Supporting Information.

include data for only the lowest energy complex at fixed values of n and q.

For a given coordination number and electronic charge, the Al−OH bond lengths are always 0.20−0.25 Å shorter than the Al−OH_2 ones. Both sets of Al−O bond lengths decrease linearly with increasing net electronic charge, as shown in Figure 4. This decrease in Al−O bond length is consistent with the contraction of the valence electron clouds with increasing net electronic charge.

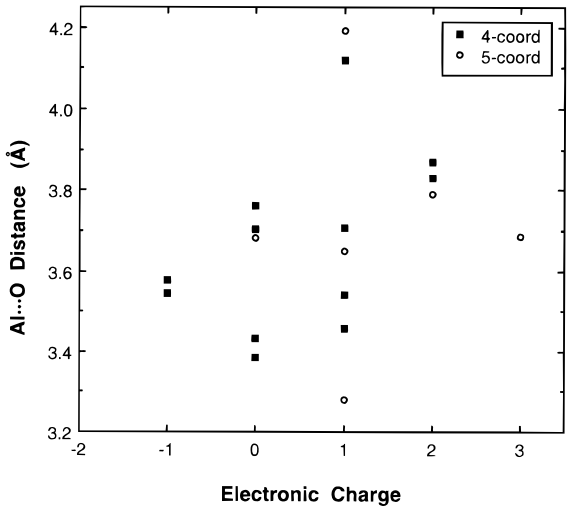

Figure 11. HF/6-31G* calculated Al···O distances as a function of the degree of protonation for $[Al(OH)_x(H_2O)_{4-x}\cdot 2H_2O]^{3-x}$ and $[Al(OH)_x(H_2O)_{5-x}\cdot H_2O]^{3-x}$ complexes.

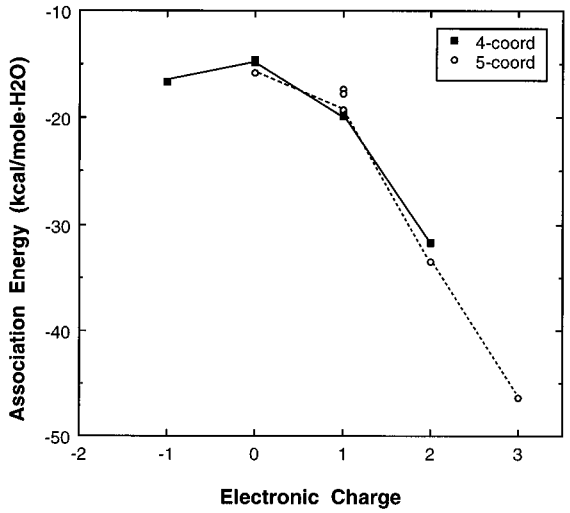

Figure 12. Association energies for $[Al(OH)_x(H_2O)_{4-x}\cdot 2H_2O]^{3-x}$ and $[Al(OH)_x(H_2O)_{5-x}\cdot H_2O]^{3-x}$ complexes as a function of the protonation level.

The orientations of the −OH and −OH_2 ligands also follow a relatively simple trend as functions of protonation (for fixed n), as shown in Figures 5 and 6. The Al−O−H bond angles of the −OH ligands increase dramatically with increasing protonation; e.g., for $n = 4$ it increases from 110.3° to 180°. The range of angles is consistent with values for other MOH systems such as HOCl molecule (H−O−Cl = 102.4°) and CsOH (Cs−O−H = 180°).[20]

We use a tilt angle to define the orientation of the −OH_2 ligand (see Scheme 1). This tilt angle is simply the angle between the Al−O bond and a plane passing through the three atoms of the H_2O ligand. The −OH_2 ligand is nucleophilic, donating a lone pair of electrons to the electropositive aluminum atom. The −OH_2 ligand has two lone pairs,[19b] a sigma pair (σ) and a pi pair (π). As shown below, bonding directly through the π lone pair would result in a tilt angle of 90°, whereas bonding through the σ pair yields a tilt angle of 0°. Tilt angles between these two extremes are consistent with hybridization

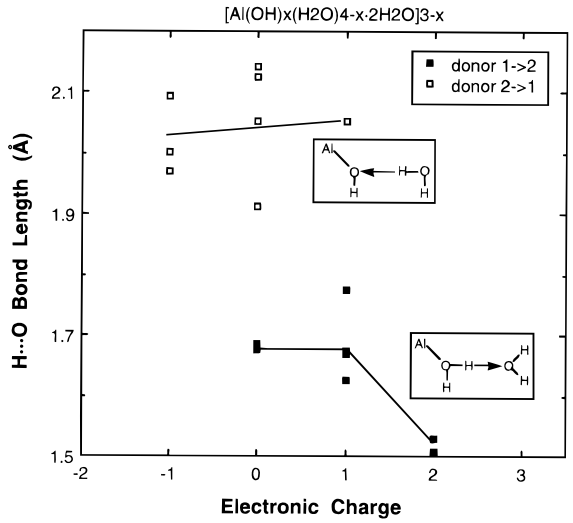

Figure 13. Hydrogen bond lengths (H···O) as a function of the protonation level for $[Al(OH)_x(H_2O)_{4-x}\cdot 2H_2O]^{3-x}$. Separate trends are shown for d1→2 and d2→1 hydrogen bonds.

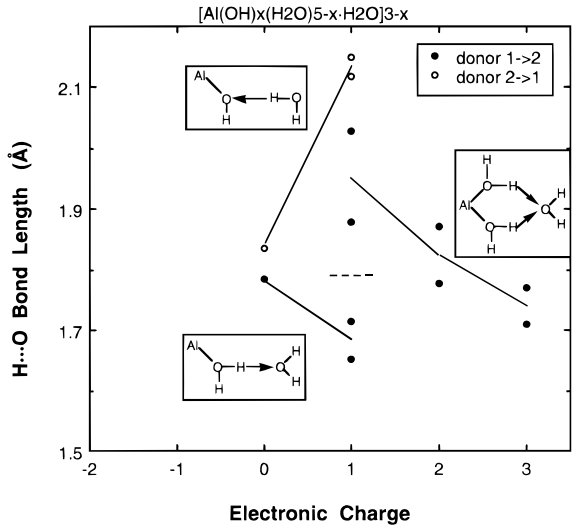

Figure 14. Hydrogen bond lengths (H···O) as a function of the protonation level for $[Al(OH)_x(H_2O)_{5-x}\cdot H_2O]^{3-x}$. Separate trends are shown for d1→2 and d2→1 hydrogen bonds.

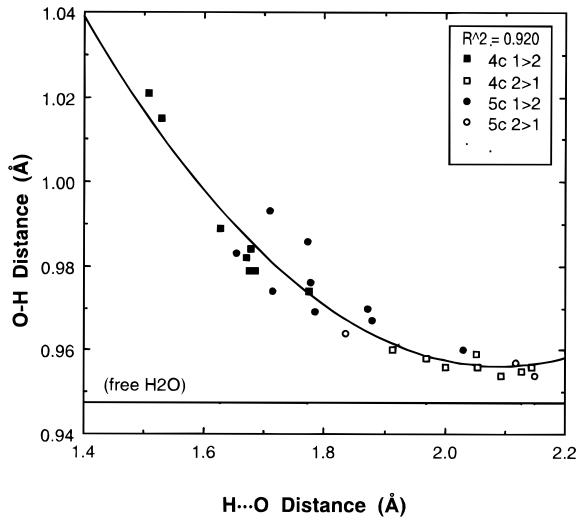

Figure 15. Correlation between O−H bond length and hydrogen bond length (H···O) for $[Al(OH)_x(H_2O)_{4-x}\cdot 2H_2O]^{3-x}$ and $[Al(OH)_x(H_2O)_{5-x}\cdot H_2O]^{3-x}$ complexes. Separate symbols are used for d1→2 and d2→1 hydrogen bonds.

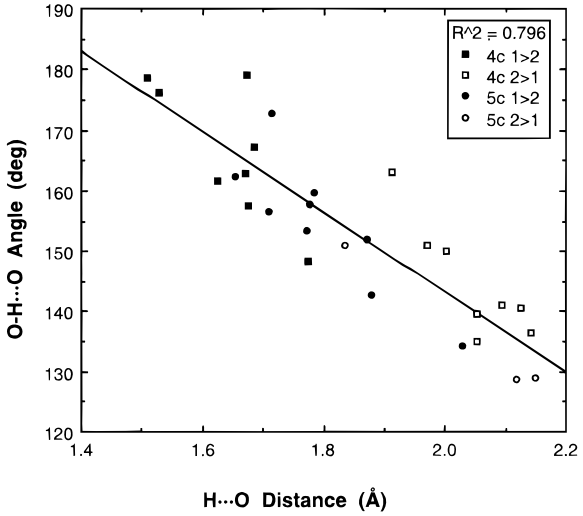

Figure 16. Correlation between O−H···O bond angle and hydrogen bond length (H···O) for $[Al(OH)_x(H_2O)_{4-x}\cdot 2H_2O]^{3-x}$ and $[Al(OH)_x(H_2O)_{5-x}\cdot H_2O]^{3-x}$ complexes. Separate symbols are used for d1→2 and d2→1 hydrogen bonds.

of the σ and π orbitals; e.g., 54.7° results from sp^3 hybridization. The H_2O tilt angle approaches zero with increasing protonation, as shown in Figure 6.

All three of these trends, Al−O bond length, Al−O−H bond angle, and Al−OH_2 tilt angle, indicate an increase in binding strength to the aluminum atom with increasing protonation.

Since the Al−O−H bond angle, the Al−OH_2 tilt angle, and the Al−O bond lengths (for −OH and −OH_2) all follow simple trends as a function of protonation, we decided to examine the relationship between the Al−OH and Al−OH_2 angles with respect to bond lengths. Figure 7 shows a 85.6% correlation between the average Al−O−H bond angles and the average Al−O bond lengths. Figure 8 indicates a 75.1% correlation between the Al−OH_2 tilt angle and the Al−O bond lengths. These correlations indicate that ligand orientations are controlled primarily by the respective Al−O bond lengths; i.e., the coordination number is of secondary importance, although it does indeed influence the Al−O bond length.

The relationship between the Al−O bond lengths (−OH and −OH_2) and the coordination number is presented in Figure 4. The calculated Al−O bond lengths increase with increasing coordination number, consistent with empirical observations for ionic crystals.[21] To simplify this comparison, we computed average Al−O bond lengths and Al^{3+} radii as functions of the coordination number by averaging the values for the lowest energy complexes in the 0, 1+, 2+, and 3+ charge states (see Table 2). The results are in reasonable agreement with Pauling's empirical ratios.[21] Using the calculated average bond lengths of Table 2 and the value of 0.675 Å for the Al^{3+} radius (n = 6),[22] we calculated radii for Al^{3+}(n = 4), Al^{3+}(n = 5), −OH (n = 1), and −OH_2 (n = 1); see Table 2. Our radii for Al^{3+}(n = 4) and Al^{3+} (n = 5) are in reasonable agreement with the empirical data,[21,22] and our radius for −OH (n = 1; 1.084 Å) is in reasonable agreement with the empirical value for −OH (n = 2; 1.18 Å).

A1. Tetrahedral Complexes, $[Al(OH)_x(H_2O)_{4-x}]^{3-x}$. The tetrahedral complexes are relatively straightforward and follow the trends stated above. Unlike the higher coordination numbers, there is only one stable structure for each level of protonation.

For $[Al(OH)_4]^-$, our calculated Al−O distance of 1.770 Å is in reasonable agreement with observed Al−O bond lengths in feldspars (1.761 Å)[23] and sodalites (1.728 Å).[24] Our $[Al(OH)_4]^-$

TABLE 1: HF/6-31G* and MP2/6-31G* Energies for Tetrahedral, Pentacoordinate, and Octahedral Aluminum Aquo−Hydroxy Complexes

complex	symmetry	HF/6-31G* energy (au)	rel energy (kcal/mol)	MP2/6-31G*//6-31G* energy (au)
		$[Al(OH)_x(H_2O)_{4-x}]^{3-x}$		
$Al(OH)_4^-$		−543.909 01		
$Al(OH)_3(H_2O)$		−544.443 47		
$Al(OH)_2(H_2O)_2^+$		−544.799 42		
$Al(OH)(H_2O)_3^{2+}$		−544.967 54		
$Al(H_2O)_4^{3+}$		−544.966 83		
		$[Al(OH)_x(H_2O)_{5-x}]^{3-x}$		
$Al(OH)_3(H_2O)_2$	[C_1]	−620.475 97	0.0	
$Al(OH)_3(H_2O)_2$	[C_s]	−620.472 48	2.2	
Al(*eq*-OH)(*ax*-OH)$(H_2O)_3^+$	[C_s]	−620.837 93	5.2	
Al(*eq*-OH)$_2(H_2O)_3^+$	[C_2]	−620.846 20	0.0	
Al(*ax*-OH)$(H_2O)_4^{2+}$	[C_s]	−621.037 96	3.4	
Al(*eq*-OH)$(H_2O)_4^{2+}$	[C_{2v}]	−621.043 32	0.0	
$Al(H_2O)_5^{3+}$	[C_{2v}]	−621.076 86		
		$[Al(OH)_x(H_2O)_{6-x}]^{3-x}$		
fac-$Al(OH)_3(H_2O)_3$	[C_3]	−696.487 49	0.0	−697.663 84
mer-$Al(OH)_3(H_2O)_3$	[C_1]	−696.483 64	2.4	
cis-$Al(OH)_2(H_2O)_4^+$	[C_2]	−696.881 21	0.0	−698.048 41
trans-$Al(OH)_2(H_2O)_4^+$	[C_{2h}]	−696.879 55	1.0	
$Al(OH)(H_2O)_5^{2+}$	[C_{2v}]	−697.105 71	1.4	
$Al(OH)(H_2O)_5^{2+}$	[C_s]	−697.108 00	0.0	−698.267 88
$Al(H_2O)_6^{3+}$	[T_h]	−697.180 91		

SCHEME 1

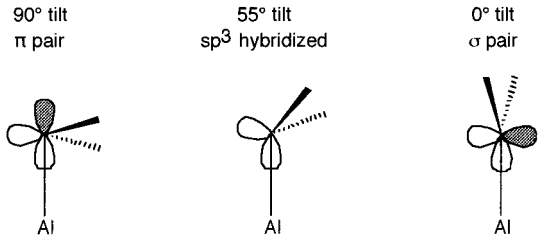

TABLE 2: Average Al−O Bond Lengths, Bond Ratios, and Al^{3+} Radii at Different Coordination Numbers

		bond ratios		Al^{3+} radii (Å)	
coord no.	av Al−O (Å)	present	Pauling[a]	present	Shannon[b]
		Al−OH			
4	1.682	0.956	0.922	0.598	0.530
5	1.710	0.972	0.964	0.626	0.620
6	1.759	1.000	1.000	0.675	0.675
		Al−OH_2			
4	1.868	0.934	0.922		
5	1.953	0.976	0.964		
6	2.000	1.000	1.000		

[a] Reference 21. [b] Reference 22.

structure is essentially identical with the symmetrical structure (S_4) calculated previously using the same basis set (6-31G*).[13] This previous study claims three minimum structures of equal energy; however, it is fairly obvious that these three degenerate structures are essentially the same symmetrical structure with different orientations in the coordinate system.

A2. Pentacoordinated Complexes, $[Al(OH)_x(H_2O)_{5-x}]^{3-x}$. For pentacoordinated species, the lowest energy complexes are those with the −OH ligands in the equatorial positions (see Figure 2). For example, the C_2 structure of $[Al(OH)_2(H_2O)_3]^+$ with both −OH ligands equatorial is 5.2 kcal/mol lower in energy than the C_s geometry with one −OH ligand axial and one equatorial. Likewise, the C_{2v} equatorial −OH isomer of $[Al(OH)_2(H_2O)_3]^{2+}$ is 3.4 kcal/mol lower in energy than the axial C_s one.

The Al−O bond lengths for the pentaaquo complex, $[Al(H_2O)_5]^{3+}$, are slightly larger than those calculated for a complex with two waters in the second hydration sphere,[25] $[Al(H_2O)_5 \cdot 2H_2O]^{3+}$. Using a double-ζ plus polarization basis set, Probst and Hermansson calculated the Al−O bond lengths to be 1.824, 1.827, and 1.914 Å, compared with the results here of 1.866, 1.873, and 1.923 Å.

A3. Octahedral Complexes, $[Al(OH)_x(H2O)_{6-x}]^{3-x}$. For the hexacoordinated complexes, the relative stabilities of isomers can be explained by the orientation of the $-OH_2$ ligands (see Figure 3). The most stable isomers tend to have the $-OH_2$ ligands oriented such that the O−H bonds eclipse an Al−OH bond. This is probably caused by an electrostatic interaction between the positive H of the $-OH_2$ ligand and the negative oxygen in −OH. For example, the facial isomer of $Al(OH)_3(H_2O)_3$ is 2.4 kcal/mol lower than the meridianal isomer where one of the $-OH_2$ ligand O−H bonds eclipses an Al−OH_2 bond. The C_s isomer of $[Al(OH)(H_2O)_5]^{2+}$ is 1.4 kcal/mol lower in energy than the C_{2v} isomer, with one extra O−H bond eclipsing an Al−OH bond in the former structure. The situation is different for $[Al(OH)_2(H_2O)_4]^+$. Here, the *cis* isomer is 1.0 kcal/mol lower than the *trans*, even though more bonds are eclipsed in the latter. What makes the difference is the ability of the $-OH_2$ ligands in the *cis* geometry to bend toward the −OH ligands and increase the favorable electrostatic interactions.

For $[Al(H_2O)_6]^{3+}$, our calculated Al−O bond length of 1.934 Å is in reasonable agreement with values of 1.865−1.923 Å observed in various alums, $MAl(SO_4)_2 \cdot 12H_2O$ (M = Na, K, NH_4, etc.; types α, β, and γ).[26] These alums all contain $[Al(H_2O)_6]^{3+}$ octahedra.

B. Complexes with Water in the Second Coordination Shell. Water molecules were added to the second coordination shells of the naked tetrahedral and pentacoordinated Al complexes of lowest energy. Two waters were added to the tetrahedral complexes and one to the pentacoordinated species so that all clusters had six oxygens. These second-shell water molecules form hydrogen bonds to the core complexes.

The HF/6-31G* energies are in Table 3. Figures 9 and 10 show the optimized geometries. For each of these structures, Cartesian coordinates, bond lengths, bond angles, and atomic charges are given in the Supporting Information. Table 4 lists geometrical parameters for the hydrogen bonds in these complexes. These parameters include the O−H bond lengths, hydrogen bond distances H···O, and the angle O−H···O. As a reference point, for ice, the hydrogen bonds have H···O

TABLE 3: Energetics for Tetrahedral and Pentacoordinated Aluminum Aquo−Hydroxy Complexes with Water in the Second Coordination Shell

complex	total energy (au) HF/6-31G*	total energy (au) MP2/6-31G*	rel energy (kcal/mol) HF	rel energy (kcal/mol) MP2	HF/6-31G* association energy (kcal/mol of 2nd-shell water)
		$[Al(OH)_x(H_2O)_{4-x}\cdot 2H_2O]$			
$[Al(OH)_4\cdot 2H_2O]^-$	−695.983 37				−16.6
$Al(OH)_3(H_2O)\cdot 2H_2O$ (complex A)	−696.511 60	−697.680 93	0.5	1.0	−14.6
$Al(OH)_3(H_2O)\cdot 2H_2O$ (complex B)	−696.512 32	−697.682 56	0.0	0.0	−14.9
$[Al(OH)_2(H_2O)_2\cdot 2H_2O]^+$ (complex A)	−696.883 96		0.1		−19.8
$[Al(OH)_2(H_2O)_2\cdot 2H_2O]^+$ (complex B)	−696.884 10	−698.045 57	0.0		−19.8
$[Al(OH)(H_2O)_3\cdot 2H_2O]^{2+}$	−697.090 29	−698.250 09			−31.8
		$[Al(OH)_x(H_2O)_{5-x}\cdot H_2O]$			
$Al(OH)_3(H_2O)_2\cdot H_2O$	−696.511 86	−697.684 25			−15.8
$[Al(OH)_2(H_2O)_3\cdot H_2O]^+$ (complex A)	−696.884 56		2.0		−17.3
$[Al(OH)_2(H_2O)_3\cdot H_2O]^+$ (complex B)	−696.885 25	−698.047 56	1.6	3.3	−17.8
$[Al(OH)_2(H_2O)_3\cdot H_2O]^+$ (complex C)	−696.887 76	−698.054 46	0.0	0.0	−19.3
$[Al(OH)(H_2O)_4\cdot H_2O]^{2+}$	−697.107 48	−698.268 84			−33.5
$[Al(H_2O)_5\cdot H_2O]^{3+}$	−697.161 63				−46.5

TABLE 4: Hydrogen Bond Geometries for Tetracoordinated and Pentacoordinated Complexes with Water in the Second Coordination Shell

H bonds	O−H (Å)	H···O (Å)	H···O−H (deg)	H bond type
		$[Al(OH)_4\cdot 2H_2O]^-$		
O5−H5···O3	0.956	2.001	150.0	d2→1 weak
O5−H5′···O6	0.952	2.217	144.6	d2→2 weak
O6−H6···O2	0.958	1.970	151.1	d2→1
O6−H6′···O3	0.954	2.093	141.1	d2→1 weak
		$[Al(OH)_3(H_2O)\cdot 2H_2O]$ (complex A)		
O4−H4···O6	0.979	1.685	167.3	d1→2
O5−H5···O3	0.956	2.053	139.5	d2→1 weak
O5−H5′···O1	0.955	2.126	140.7	d2→1 weak
O6−H6···O5	0.967	1.824	164.4	d2→2
		$[Al(OH)_3(H_2O)\cdot 2H_2O]$ (complex B)		
O4−H4···O5	0.984	1.676	157.6	d1→2
O5−H5···O3	0.956	2.143	136.4	d2→1 weak
O5−H5′···O6	0.960	1.952	156.1	d2→2
O6−H6···O1	0.960	1.912	163.0	d2→1
		$[Al(OH)_2(H_2O)_2\cdot 2H_2O]^+$ (complex A)		
O3−H3···O5	0.974	1.774	148.4	d1→2
O4−H4···O6	0.982	1.670	162.8	d1→2
O5−H5···O1	0.959	2.052	135.0	d2→1 weak
O6−H6···O5	0.954	2.119	147.5	d2→2 weak
		$[Al(OH)_2(H_2O)_2\cdot 2H_2O]^+$ (complex B)		
O3−H3···O6	0.979	1.674	179.1	d1→2
O4−H4···O5	0.989	1.625	161.7	d1→2
O5−H5···O2	0.953	2.252	125.2	d2→1 weak
		$[Al(OH)(H2O)_3\cdot 2H_2O]^{2+}$		
O2−H2···O6	1.021	1.508	178.6	d1→2
O4−H4···O5	1.015	1.528	176.3	d1→2
		$[Al(OH)_3(H_2O)_2\cdot H_2O]$		
O4−H4···O6	0.969	1.784	159.8	d1→2
O6−H6···O3	0.964	1.836	150.9	d2→1
		$[Al(OH)_2(H_2O)_3\cdot H_2O]^+$ (complex A)		
O5−H5···O6	0.983	1.653	162.5	d1→2
O6−H6···O1	0.954	2.149	128.9	d2→1 weak
		$[Al(OH)_2(H_2O)_3\cdot H_2O]^+$ (complex B)		
O5−H5···O6	0.974	1.714	172.9	d1→2
		$[Al(OH)_2(H_2O)_3\cdot H_2O]^+$ (complex C)		
O3−H3···O6	0.967	1.879	142.8	d1→2
O6−H6···O2	0.958	2.118	128.8	d2→1 weak
O5−H5···O6	0.960	2.029	134.3	d1→2 weak
		$[Al(OH)(H_2O)_4\cdot H_2O]^{2+}$		
O2−H2···O6	0.976	1.777	157.8	d1→2
O5−H5···O6	0.970	1.871	152.0	d1→2
		$[Al(H_2O)_5\cdot H_2O]^{3+}$		
O1−H1···O6	0.993	1.710	156.6	d1→2
O4−H4···O6	0.986	1.771	153.4	d1→2

distances of 1.74 Å, O−H distances of 1.01 Å, and strengths of roughly 5.5 kcal/mol.[27]

The various hydrogen bonds exhibited by the aluminum aquo−hydroxy clusters can be classified according to the coordination shells of the proton donor and proton acceptor. As an example, a hydrogen bond donating a proton from the first shell into the second shell is denoted d1→2. This notation is used throughout this paper, including several tables and figures. Three types of hydrogen bonds are exhibited: d1→2, d2→1, and d2→2.

For each case, i.e., combination of coordination number and degree of protonation, there are several likely possibilities for orientations of the waters in the second coordination shell. In general, we attempted to find the lowest energy complexes. The lowest energy structures had the following hydrogen-bonding properties: (1) maximum number of hydrogen bonds between the first and second shells, d1→2 and d2→1 types; (2) multiple bonding of second shell waters (up to three hydrogen bonds each); (3) $-OH_2$ ligands act as proton donors (d1→2) but not as proton acceptors (no d2→1); (4) −OH ligands act as proton acceptors (d2→1) but not as proton donors (no d1→2).

Details of these observations are examined later in this section. In addition, we imposed the conditions that (5) first-shell waters donate only one proton and (6) second-shell waters occur on the same side of the complex.

Conditions 4 and 5 ensure that the Al−OH and Al−O(H)H fragments in these complexes model the Al−OSi and Al−O(H)-Si fragments in zeolites. Condition 4 is satisfied naturally as a consequence of energy minimization. Condition 6 is relatively unimportant but was imposed since some zeolite frameworks tend to exclude contiguous regions of the second coordination sphere. The relatively minor limitations (5 and 6) on the hydrogen bonding ensure that the complexes serve as the simplest models for studying the different coordination states of aluminum sites in zeolite frameworks.

We examined several but not all possible orientations of the second-shell waters. The structures obtained under these conditions are expected to have total energies no more than 0.5 kcal/mol higher than any structures not allowed by these conditions or any structures we may have missed. Hence, the main results of this paper should not be affected by the imposed conditions.

We first compare our results for the model complexes with two experimental crystal structures of molecular sieves where the water oxygen positions are known. We then describe the details of the hydrogen bonding and the dependence of the hydrogen bonding on the level of protonation and on the coordination number. Several general correlations on hydrogen bond geometries and strengths are observed. Finally, several specific cluster isomers are examined in further detail.

Figure 11 shows the distances between the second-shell water molecules and the aluminum center as a function of the net electronic charge of the cluster. These Al···O distances do not exhibit any obvious trends with respect to cluster charge or coordination number, except that shorter Al···O distances are allowed for tetracoordinated clusters in comparison with pentacoordinated clusters. The Al···O distances exhibit a wide range of values, ranging from 3.3 to 4.2 Å. For $[Al(OH)_4 \cdot 2H_2O]^-$, the calculated Al···O distances of 3.54 and 3.58 Å are in reasonable agreement with observed Al···O distances of 3.9−4.3 Å for a hydrated zeolite Li−A(BW)[28] and with the observed Al···O distances of 3.9, 4.2, and 4.4 Å for the large-pore hydrated aluminophosphate VPI-5.[29] Note that the waters are perturbed by cations in Li−A(BW) but not in VPI-5 or the cluster models.

Figure 12 and Table 3 show the calculated association energies as functions of the protonation level, that is, the energetics for the following reactions:

$$[Al(OH)_x(H_2O)_{4-x}]^{3-x} + 2H_2O \rightarrow [Al(OH)_x(H_2O)_{4-x} \cdot 2H_2O]^{3-x}$$

$$[Al(OH)_x(H_2O)_{5-x}]^{3-x} + H_2O \rightarrow [Al(OH)_x(H_2O)_{5-x} \cdot H_2O]^{3-x}$$

These complexation energies include components due to directional hydrogen bonding and due to long-range electrostatic interactions, e.g., the interactions of the dipole moments of the second-shell waters with the atomic charges within the first-shell core. The energies of association (per mole of second shell water) are very similar between the tetrahedral and pentacoordinated complexes. Association strengthens dramatically as the level of protonation is increased, except for $[Al(OH)_4 \cdot 2H_2O]^-$, which has a slightly stronger association energy than $[Al(OH)_3(H_2O) \cdot 2H_2O]$. For clusters with charges of 0, +1, +2, and +3, the average association energies are −15.1, −18.8, −32.7, and −46.5 kcal/(mol of second-shell water), respectively. For the +2 and +3 cases, the hydrogen bonds have H···O distances ranging from 1.51 to 1.87 Å, and they are all of the d1→2 type. The additional stabilization found in these cases indicates that the hydrogen bonds are approaching strengths that would lead to proton transfer,

$$[Al(OH)(H_2O)_3 \cdot 2H_2O]^{2+} \rightarrow [Al(OH)_2(H_2O)_2 \cdot H_2O \cdot H_3O]^{2+}$$

$$[Al(OH)(H_2O)_3 \cdot 2H_2O]^{2+} \rightarrow [Al(OH)_3(H_2O) \cdot 2H_3O]^{2+}$$

The increase of complex stabilization with increasing level of protonation is due to two factors. As an aid in discussing these two factors, we show the hydrogen bond distance H···O as a function of the net electronic charge for the four- and five-coordinate clusters in Figures 13 and 14, respectively. The major factor is that, as the protonation level increases, longer, weaker d2→1 hydrogen bonds are replaced by shorter, stronger d1→2 hydrogen bonds. In addition, these d1→2 bonds become stronger and shorter with increasing levels of protonation. On the other hand, the weaker d2→1 bonds do not appear to follow any obvious trends as far as bond strength or bond length with respect to the level of protonation.

For the tetrahedral clusters, the H···O hydrogen bond distances are similar for the neutral and +1 cases but much shorter for the +2 case, 1.68−1.69, 1.63−1.77, and 1.51−1.53 Å, respectively. For $[Al(OH)(H_2O)_3 \cdot 2H_2O]^{2+}$, these H···O distances approach the range for proton-transfer transition states,

SCHEME 2

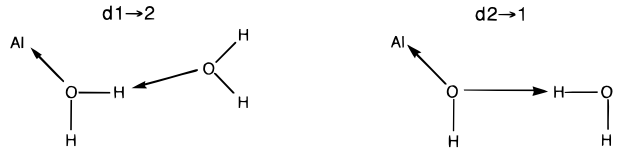

suggesting that $[Al(OH)(H_2O)_3 \cdot 2H_2O]^{2+}$ may be susceptible to proton transfer, to, for example, $[Al(OH)_2(H_2O)_2 \cdot H_2O \cdot H_3O]^{2+}$. For the pentacoordinated clusters, the hydrogen bond distances are very similar, except for the +1 isomers where many different hydrogen bonding arrangements are present. The d1→2 O···H distances vary from 1.65 to 1.88 Å, depending on the number of hydrogen bonds between the first and second shells. The more hydrogen bonds in the complex, the longer the calculated O···H distances.

Generally, we find that the stronger the hydrogen bond, the shorter the H···O distance, the longer the O−H bond length, and the closer the O−H···O angle approaches 180°. The correlations of O−H bond length and O−H···O angle with the H···O distance are shown in Figures 15 and 16. These figures include H···O distances ranging from 1.5 to 2.2 Å, in the range of hydrogen bonds in carbohydrates (1.7−2.2 Å).[30,31] Hydrogen bonds having distances H···O > 2.2 Å tend to be rather weak.[30,31] We use the following geometrical parameters as guides to characterize hydrogen bonds as strong or weak. A strong hydrogen bond has H···O < 2.0 Å, O−H···O > 150°, and O−H > 0.96 Å. Weak hydrogen bonds have H···O > 2.0 Å and O−H < 0.96 Å.

Figures 15 and 16 use different symbols to distinguish between d1→2 and d2→1 hydrogen bonds. Here, it is clear that the d1→2 bonds tend to be stronger than the d2→1 bonds—they have shorter H···O distances, longer O−H distances, and wider O−H···O angles. Using H···O = 2.0 Å as a dividing point, the weak hydrogen bonds are labeled in Table 4. All but three of the d2→1 hydrogen bonds have H···O > 2.0 Å, while all but one of the d1→2 hydrogen bonds have H···O < 1.9 Å. Based on the hydrogen bond geometries, the strengths of hydrogen bonds in these clusters follow the general trend d1→2 > d2→1 > d2→2. The d1→2 hydrogen bonds always involve donation from the Al−OH_2 protons and never from the Al−OH protons. d2→1 hydrogen bonds always donate into −OH ligands and never into −OH_2 ligands.

The d1→2 and d2→1 hydrogen bonds induce significant distortions on the core structure geometries. These distortions are best understood in terms of perturbations of the chemical bonding of the first shell −OH and −OH_2 ligands that are directly involved in hydrogen bonding. The chemical bonding can be discussed from a covalent reference point, where −OH ligands pull electron density away from a neutral aluminum or from an ionic reference point, where hydroxide anions donate electron density into Al^{3+} valence orbitals. We chose the ionic reference point for this discussion, since the calculated charge on the aluminum is +1.3*e* to +2.6*e* for these systems (see Supporting Information). Water ligands (−OH_2) carry positive charge and donate electron density to the aluminum. The −OH ligands are stronger electron donors than the −OH_2 ligands, and they also bind more strongly to the aluminum. All other factors being equal, i.e., coordination number, site (axial vs equatorial) and electronic charge, the Al−OH bond lengths are 0.20−0.25 Å shorter than the Al−OH_2 ones.

The diagrams in Scheme 2 are useful in explaining how hydrogen bonds perturb the chemical bonding of the first shell −OH and −OH_2 ligands. Here, arrows are used to show electron donation. d1→2 hydrogen bonding decreases the Al−O

TABLE 5: HF/6-31G* and MP2/6-31G* (in Parentheses) Relative Energies (kcal/mol) between Al^{3+} Complex Isomers of Different Coordination

charge	tetrahedral	pentacoordinate	octahedral
−1	$[Al(OH)_4 \cdot 2H_2O]^-$	$[Al(OH)_4(H_2O) \cdot H_2O]^-$	$Al(OH)_4(H_2O)_2^-$
	0.0	not stable	not stable
0	$Al(OH)_3(H_2O) \cdot 2H_2O$	$Al(OH)_3(H_2O)_2 \cdot H_2O$	$Al(OH)_3(H_2O)_3$
	0.0 (1.1)	0.3 (0.0)	15.6 (12.8)
+1	$[Al(OH)_2(H_2O)_2 \cdot 2H_2O]^+$	$[Al(OH)_2(H_2O)_3 \cdot H_2O]^+$	$Al(OH)_2(H_2O)_4^+$
	2.3 (5.5)	0.0 (0.0)	4.1 (3.8)
+2	$[Al(OH)(H_2O)_3 \cdot 2H_2O]^{2+}$	$[Al(OH)(H_2O)_4 \cdot H_2O]^{2+}$	$Al(OH)(H_2O)_5^{2+}$
	11.1 (11.8)	0.3 (0.0)	0.0 (0.6)
+3	$[Al(H_2O)_4 \cdot 2H_2O]^{3+}$	$[Al(H_2O)_5 \cdot H_2O]^{3+}$	$Al(H_2O)_6^{3+}$
	not stable	12.1	0.0

bond lengths in Al−OH_2. Second-shell waters stabilize the positive charge on −OH_2, thus increasing its binding and electron donation to the aluminum. As an example, for $[Al(OH)_3(H_2O) \cdot 2H_2O]$ (complex B), the Al−OH_2 bond length and tilt angle are 1.92 Å and 45.9°, as compared to 1.98 Å and 61.7° for the naked complex. This type of hydrogen bonding is very important for the stabilization of complexes with net positive charges.

d2→1 hydrogen bonding increases the Al−O bond lengths in Al−OH. Second-shell waters decrease the electron donation of the hydroxide anion and decrease its binding to the aluminum. For $[Al(OH)_3(H_2O) \cdot 2H_2O]$ (complex B), two of the three −OH ligands participate in d2→1 hydrogen bonding, whereas the third is unperturbed. In comparison with the unperturbed −OH ligand, the two −OH ligands that accept d2→1 hydrogen bonds have longer Al−O bond lengths (∼0.020 Å) and narrower Al−O−H bond angles (shorter by 3.1°).

B1. Second-Shell Water Arrangements. The concept of weak and strong hydrogen bonds can explain the relative stabilities of various clusters that differ in the arrangement of the second-shell water molecules. The energy differences between isomers having the same coordination number is small (less than 0.5 kcal/mol), mainly due to the fact that the number of hydrogen bonds is usually constant. Two sets of tetrahedral isomers and one set of pentacoordinated isomers are available for comparison. Figures 9 and 10 show structures for these complexes; structural parameters for the hydrogen bonds are given in Table 4.

B2. Tetrahedral Complexes, $[Al(OH)_x(H_2O)_{4-x} \cdot 2H_2O]^{3-x}$. For the $[Al(OH)_3(H_2O) \cdot 2H_2O]$ isomers, complex B is 0.5 kcal/mol more stable than complex A. Each isomer contains four hydrogen bonds: one strong d1→2, two d2→1, and one d2→2. The main difference is that, in the higher energy isomer, both d2→1 bonds are donated from the same second-shell water, whereas in the lower energy isomer, each second-shell water donates into one d2→1 bond. This is consistent with the observation that, for complex A, both d2→1 bonds are "weak" (H···O = 2.05 and 2.13 Å) whereas complex B has one weak and one "strong" d2→1 bond (H···O = 1.91 and 2.14 Å).

For $[Al(OH)_2(H_2O)_2 \cdot 2H_2O]^+$, complex B is 0.1 kcal/mol lower than complex A, even though it has one fewer hydrogen bond (three vs four). This is consistent with the observation that the d1→2 bonds of complex B (H···O = 1.63 and 1.67 Å) are stronger than those of complex A (H···O = 1.67 and 1.77 Å). For $[Al(OH)_2(H_2O)_2 \cdot 2H_2O]^+$, it appears that forming an additional weak d2→2 hydrogen bond as in complex A (H···O = 2.12 Å) requires distorting and weakening the d1→2 bonds.

No stable structures corresponding to $[Al(H_2O)_4 \cdot 2H_2O]^{3+}$ were found. Optimization of an initial $[Al(H_2O)_4 \cdot 2H_2O]^{3+}$ structure led to proton transfers yielding clusters with second-shell hydronium cations, such as $[Al(OH)_2(H_2O)_2 \cdot 2H_3O]^{3+}$. This deprotonation tendency has been observed before[25] and is consistent with the anomalously strong hydrogen bonds observed in the tetrahedral cluster $[Al(OH)(H_2O)_3 \cdot 2H_2O]^{2+}$ (H···O = 1.51 and 1.53 Å; see the previous section).

B3. Pentacoordinated Complexes, $[Al(OH)_x(H_2O)_{5-x} \cdot H_2O]^{3-x}$. In the case of pentacoordinated clusters, structural variations can result from both second-shell water arrangements as well as arrangements of the first-shell ligands in axial and equatorial positions. As shown in section IVA, the most stable naked complexes involve placing the electron-donating water ligands in the equatorial positions. We find that the most stable complexes tend to exhibit equatorial d1→2 hydrogen bonds that increase equatorial electron donation. The results below indicate that equatorial d1→2 bonds are favored over axial d1→2 bonds because of the need to increase equatorial electron donation into aluminum.

For $[Al(OH)_2(H_2O)_3 \cdot H_2O]^+$, three stable isomers were obtained: A, B, and C. Complex C is the most stable isomer, with two d1→2 hydrogen bonds and one d2→1 hydrogen bond. In complex C, the equatorial d1→2 bond (H···O = 1.88 Å) is stronger than the axial d1→2 bond (H···O = 2.03 Å). Complex B is less stable than complex C by only 3.3 kcal/mol (at the MP2/6-31G* level) even though it contains just one hydrogen bond! The hydrogen bond of complex B is a very strong equatorial d1→2 bond (H···O = 1.71 Å) that increases equatorial electron donation into the aluminum. Complex A is less stable than complex B by 0.4 kcal/mol (at the HF/6-31G* level), even though it contains one more hydrogen bond and even though its axial d1→2 bond (H···O = 1.65 Å) is shorter than the equatorial d1→2 bond of complex B.

$[Al(OH)(H_2O)_4 \cdot H_2O]^{2+}$ and $[AlH_2O)_5H_2O]^{3+}$ each contain two d1→2 hydrogen bonds. In each case, the equatorial d1→2 bond is 0.06−0.10 Å shorter than the axial d1→2 bond.

No stable structures corresponding to $[Al(OH)_4(H_2O) \cdot H_2O]^-$ were found. Attempts at optimizing $[Al(OH)_4(H_2O) \cdot H_2O]^-$ led to tetrahedral geometries with two molecules in the second coordination shell, $[Al(OH)_4 \cdot 2H_2O]^-$. This suggests a strong preference for tetrahedral coordination for anionic aluminum clusters.

C. Energetics for Transformations of Coordination Number. Energies for the various Al complexes, $[Al(OH)_x(H_2O)_{n-x} \cdot mH_2O]^{3-x}$, $n + m = 6$, are given in Tables 1, 3, and 5. In these tables, the complexes are listed in order of increasing net cluster charge, $q = 3 - x$. As the protonation level increases, −OH ligands are replaced by −OH_2 ligands, which carry the positive charge. Note that each value of q ($q = -1$, 0, +1, +2, and +3) identifies a particular set of isomers having aluminum coordination numbers of $n = 4$, 5, and 6. To examine the energetics for transformation of coordination number as a function of q, we take the most stable (lowest energy) complex for each value of n and calculate the relative energies. These relative energies are displayed in Table 5 and Figure 17 as a function of q.

In several cases, especially for $q = +1$, the relative energies of various isomers were quite close as calculated at the HF/6-

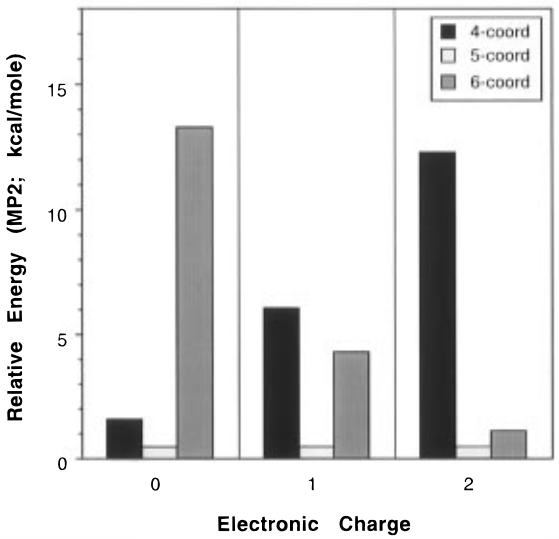

Figure 17. Relative energies of tetrahedral, pentacoordinated, and octahedral isomers as a function of the degree of protonation as calculated at the MP2/6-31G*//HF/6-31G* level. The tetrahedral and pentacoordinated complexes contain two and one second-shell waters, respectively.

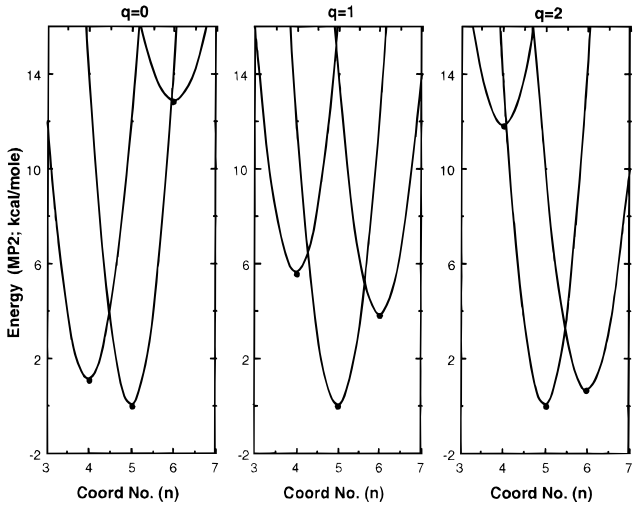

Figure 18. Energy curves governing transformations of coordination for protonation levels $q = 0$, $q = +1$, and $q = +2$.

31G* level. To test the sensitivity of the results to the level of the calculation, we used a more sophisticated level of calculation called MP2/6-31G* (i.e., MP2/6-31G*//HF/6-31G*; see section III). The overall trends in stabilities calculated at these two levels of theory are similar, although the HF/6-31G* calculations appear to be biased by up to 2.8 kcal/mol against the higher coordination clusters, particularly $n = 6$. In this discussion, for $q = 0$, $+1$, and $+2$, we use the relative energies calculated at the MP2/6-31G* level. For $q = -1$ and $q = +3$, the HF/6-31G* results were good enough. Tables 1, 3, and 5 list results for both HF/6-31G* and MP2/6-31G*.

As the degree of protonation increases, the preferred coordination number increases from four to six, as shown in Figure 17. For $q = -1$, the only stable isomer was the tetrahedral complex, $[Al(OH)_4 \cdot 2H_2O]^-$. Here, upon structural optimization, initial pentacoordinate and octahedral structures corresponding to $[Al(OH)_4(H_2O) \cdot H_2O]^-$ and $[Al(OH)_4(H_2O)_2]^-$, respectively, were unstable and transformed to $[Al(OH)_4 \cdot 2H_2O]^-$. For $q = 0$, $n = 5$ is slightly more stable than $n = 4$, but $n = 6$ is substantially less stable. For $q = +1$, the preferred coordination is $n = 5$, but the octahedral complex is now 1.7 kcal/mol below the tetrahedral complex. For $q = +2$, $n = 5$ is only slightly more stable than $n = 6$, but $n = 4$ is substantially less stable. For $q = +3$, $n = 6$ is 12 kcal/mol more stable than $n = 5$, and $n = 4$ species is completely unstable; i.e., upon optimization, $n = 4$ complexes transform to $n = 5$ or $n = 6$.

In Figure 18, we present the relative energies of the different coordinations using Bell−Evans−Polyani (BEP) diagrams.[32] A diagram is given for isomers of 0, +1, and +2, net charge. The BEP diagrams illustrate qualitatively how the differences in energy affect the interconversion between species. For example, as the energy difference between the tetrahedral and pentacoordinate species becomes more exothermic, the barrier to isomerization decreases. Transformation from tetrahedral to octahedral coordination is shown to be difficult for the $q = 0$ case where the octahedral cluster is high in energy but is easier for the species with $q = 1$. Indeed, for the case of $q = 2$, the change from tetrahedral to octahedral coordination should be favored. In all cases, the relatively low energy of the five-coordinate species allows for a facile transformation to octahedral coordination.

To test the sensitivity of the results on the number of waters chosen, we reinvestigated the cases of $q = 0$ with one fewer water molecule in the tetrahedral and pentacoordinated complexes. The tetracoordinated complex $[Al(OH)_3(H_2O) \cdot H_2O]$ is calculated to be 2.1 kcal/mol *lower* in energy at the MP2/6-31G* level than the pentacoordinated one $[Al(OH)_3(H_2O)_2]$, a reversal of the case with one extra water (see above). This is consistent with our observations on the importance of d1→2 hydrogen bonds in stabilizing first-shell water ligands. Hence, excess water is important in stabilizing the higher coordinated species. For optimum stability, each first-shell water ligand ($Al-OH_2$) requires 1−2 second-shell water molecules.

Discussion

The main results of this paper are given in Figures 12, 15, 17, and 18. Figure 12 shows that the association energies can be quite strong, especially as the level of protonation increases. The association energies range from −15 to −46 kcal/(mol of second-shell water). Figures 13−15 shows that the d1→2 hydrogen bonds are substantially stronger than d2→1 hydrogen bonds. This is not a surprising result, since the protons from $Al-OH_2$ ligands are highly acidic, and these protons are the donors for d1→2 hydrogen bonds.

Figures 17 and 18 show that transformations involving changes of coordination number do not require large energies. Each of the protonation levels with net complex charge $0 \le q \le +2$ has a range of stable coordination numbers, which are within 1−5 kcal/mol of the lowest energy species. For $q = -1$, the only stable coordination number is four. For $q = 0$, the stable coordination numbers are four and five. For $q = +1$ and +2, five and six are the stable n values, and for $q = +3$, $n = 6$ is the only stable coordination number. The trends suggest that expanding or contracting the coordination environment by one ligand can be a facile process for species having net complex charges in the range $0 \le q \le +2$.

Energies needed for coordination transformations (Figures 17 and 18) are substantially smaller than the hydrogen bond energies (Figure 12). Therefore, variations of the amount of water within the second-shell coordination sphere of the aluminum will affect the relative stability of different aluminum coordinations. In particular, it appears that each first-shell water ligand ($Al-OH_2$) requires at least one second-shell water for optimum stability.

With increasing levels of protonation, the shift in preference from tetrahedral to octahedral coordination appears to be due to the need for stabilizing the increasing positive charge on the

Al center. This is evidenced by the decrease in the d1→2 O···H bond lengths as the cluster charges increase, especially for $q = +2$ and $+3$ (see Figures 13 and 14). The shorter d1→2 hydrogen bonds facilitate greater electron donation from the first shell ligands to the aluminum cation.

For the higher charged complexes, increasing the coordination number allows for better stabilization of charge. For example, in the isomers where $q = +2$, the pentacoordinated isomer is 11.8 kcal/mol lower in energy than the tetrahedral isomer. This is consistent with the observation that adding waters to the first coordination shell is more effective in stabilizing the positive aluminum charge than adding waters to the second coordination shell. Indeed, during the optimization of tetrahedral complexes with $q > 0$, if the second shell waters were not participating in d1→2 hydrogen bonds increasing the electron donation of the first shell ligands, the second shell waters entered the first shell.

Excess water is obviously needed to create the higher coordination Al complexes and as shown above stabilize the more positively charged complexes. But additional water may also favor formation of higher coordination in complexes with moderate charge. As seen for the complexes with $q = 0$, the addition of another water molecule in the second shell changes the coordination preference from four to five. In the pentacoordinated complex $[Al(OH)_3(H_2O)_2 \cdot H_2O]$, the extra water hydrogen bonds to the $-OH_2$ ligand (d1→2) and stabilizes the complex. The excess water requirement is consistent with experiments on H−rho zeolite, where octahedral peaks in the ^{27}Al NMR disappear under anhydrous conditions.[1]

The results presented in section C suggest that pentacoordinated or octahedral Al species within a zeolite framework could be produced under conditions of high acidity and sufficient water content, i.e., $n = 5$ for $q = 0$ or $q = +1$ and $n = 6$ for $q = +1$. Because the calculated energy differences between different coordinations can be small, additional factors may affect the relative stability of Al coordinations, such as strain energy induced by the framework, and the amount of available water.

The results should be reasonably accurate for these cluster models. However, we have several concerns on how well the clusters represent aluminum sites in zeolites. First, the clusters have considerably more conformational freedom than aluminum sites within zeolites; e.g., embedding these clusters in a zeolite framework would require significant bond angle distortions. Also, in these clusters, hydroxy groups were used to model siloxy groups. Finally, we chose an arbitrary amount of water, i.e., $[Al(OH)_x(H_2O)_{n-x} \cdot mH_2O]^{3-x}$ with $n + m = 6$. We tested this in one case where $n + m = 5$ gave similar results as $n + m = 6$, but further work with $n + m > 6$ could be beneficial, since the association energies are significantly greater than the energies for transformation of the aluminum coordination. For optimum stability, each first-shell water ligand ($Al-OH_2$) will require 1−2 second-shell water molecules.

Conclusions

Structures and energies were calculated for Al hydroxy−aquo complexes having coordination numbers $n = 4$, 5, and 6. These complexes served as the simplest models of Al sites in zeolites. The relative stabilities of the different coordinations were determined as functions of the degree of protonation, at the oxygen sites in the clusters. The transformation of Al from tetrahedral to octahedral coordination is important because it determines the acidity of zeolites. The presence of octahedral aluminum species may also contribute to pore plugging and to decomposition of zeolite catalysts.

The shift in preference from tetrahedral to octahedral coordination occurs when the net charge on the complex, q, is equal to $+1$ (see Figure 17). Here the octahedral complex is calculated to be 1.7 kcal/mol lower in energy than the tetrahedral one. For complexes with $q \geq +1$, octahedral coordination is preferred over tetrahedral coordination. For $0 \leq q \leq +2$, the pentacoordinate species were most stable.

Hydrogen bonding between the first and second coordination shells is found to be very important. The d1→2 hydrogen bonds, involving the highly acidic $Al-OH_2$ protons, are substantially stronger than d2→1 hydrogen bonds, where the second-shell waters donate into the Al−OH ligands. Hydrogen bonds are very important in stabilizing the five- and six-coordinate species, especially for the highly protonated complexes. For optimum stability, each first-shell water ligand ($Al-OH_2$) requires 1−2 second-shell water molecules. As a result, excess water is needed to produce higher coordinated aluminum species.

Trends in bond lengths, angles, and ligand orientations were identified as functions of coordination number and complex charge. Cartesian coordinates for all species were tabulated and can be used in future studies to assist the parametrization of Al sites in framework models of zeolites.

Acknowledgment. We acknowledge helpful discussions with Dr. Patricia Andreozzi and Prof. C. R. A. Catlow.

Supporting Information Available: Cartesian coordinates, atomic partial charges, and relevant interatomic distances for all optimized geometries (33 pages). Ordering information is given on any current masthead page.

References and Notes

(1) Vega, A. J.; Luz, Z. *J. Phys. Chem.* **1987**, *91*, 365.

(2) Garces, J. Unpublished results.

(3) *Comprehensive Coordination Chemistry. The Synthesis, Reactions, Properties, and Applications of Coordination Compounds*; Wilkinson, G., Ed.; Pergamon: New York, 1987; Vol. 3, Chapter 25. Aluminum and Gallium. 25.1.5 Oxygen ligands, p 112.

(4) Cotton, F. A.; Wilkinson, G. *Advanced Inorganic Chemistry*, 5th ed.; Wiley: New York, 1988; p 215.

(5) Pelmenschikov, A. G.; Morosi, G.; Gamba, A. *J. Phys. Chem.* **1992**, *96*, 7422.

(6) Sauer, J. In *Modeling of Structure and Reactivity in Zeolites*; Catlow, C. R. A., Ed.; Academic Press: New York, 1992.

(7) Veillard, H.; Demuynck, J.; Veillard, A. *Chem. Phys. Lett.* **1975**, *33*, 221. Veillard, H. *J. Am. Chem. Soc.* **1977**, *99*, 7194.

(8) Hariharan, P. C.; Pople, J. A. *Theor. Chim. Acta* **1973**, *28*, 212.

(9) Nicholas, J. B.; Winans, R. E.; Harrison, R. J.; Iton, L. E.; Curtiss, L. A.; Hopfinger, A. J. *J. Phys. Chem.* **1992**, *96*, 7958.

(10) Nicholas, J. B.; Winans, R. E.; Harrison, R. J.; Iton, L. E.; Curtiss, L. A.; Hopfinger, A. J. *J. Phys. Chem.* **1992**, *96*, 10247.

(11) Sauer, J.; Horn, J.; Häser, M.; Ahlrichs, R. *Chem. Phys. Lett.* **1990**, *173*, 26.

(12) Brand, H. V.; Curtiss, L. S.; Iton, L. E. *J. Phys. Chem.* **1992**, *96*, 7725.

(13) De Almeida, W. B.; O'Malley, P. J. *J. Mol. Struct. (THEOCHEM)* **1992**, *257*, 305.

(14) Teunissen, E. H.; van Duijneveldt, F. B.; van Santen, R. A. *J. Phys. Chem.* **1992**, *96*, 366.

(15) The SPARTAN electronic structure program is available from Wavefunction, Inc., 18401 Von Karman Ave., Suite 210, Irvine, CA 92715.

(16) GAUSSIAN 92; Frisch, M. J.; Trucks, G. W.; Head-Gordon, M.; Gill, P. M. W.; Wong, M. W.; Foresman, J. B.; Johnson, B. G.; Schlegel, H. B.; Robb, M. A.; Replogle, E. S.; Gomperts, R.; Andres, J. L.; Raghavachari, K.; Binkley, J. S.; Gonzalez, C.; Martin, R. L.; Fox, D. J.; Defrees, D. J.; Baker, J.; Stewart, J. J. P.; Pople, J. A. Gaussian, Inc.: Pittsburgh, PA, 1992.

(17) Dewar, M. J. S.; Zoebisch, E. G.; Healy, E. F.; Stewart, J. J. P. *J. Am. Chem. Soc.* **1985**, *107*, 3902. Dewar, M. J. S.; Holder, A. J. *Organometallics* **1990**, *9*, 508.

(18) Møller, C.; Plesset, M. S. *Phys. Rev.* **1936**, *46*, 618. Pople, J. A.; Binkley, J. S.; Seeger, R. *Int. J. Quantum Chem.* **1976**, *S10*, 1.

(19) (a) Hehre, W. J.; Radom, L.; Schleyer, P. v. R.; Pople, J. A. *Ab Initio Molecular Orbital Theory*; John Wiley and Sons: New York, 1986. (b) Kettle, S. F. A. *Symmetry and Structure*, John Wiley and Sons: New York, 1985.

(20) Harmony, M. D.; Laurie, V. W.; Kuczkowski, R. L.; Schwendeman, R. H.; Ramsay, D. A.; Lovas, F. J.; Lafferty, W. J.; Maki, A. G. *J. Phys. Chem. Ref. Data* **1979,** *8*, 619.

(21) Pauling, L. *The Nature of the Chemical Bond*, 3rd ed.; Cornell University Press: New York, 1960.

(22) Shannon, R. D.; Prewitt, C. T. *Acta Crystallogr.* **1969,** *B25*, 925.

(23) Jones, J. B. *Acta Crystallogr.* **1968**, *B24*, 355.

(24) Depmeier, W. *Acta Crystallogr.* **1987**, *C43*, 2251. Lons, V. J. ; Schulz, H. *Acta Crystallogr.* **1967**, *23*, 434.

(25) Probst, M. M.; Hermansson, K. *J. Chem. Phys.* **1992**, *96*, 8995.

(26) Larson, A. C.; Cromer, D. T. *Acta Crystallogr.* **1967**, *22*, 793.

(27) Eisenberg, D.; Kauzmann, W. *The Structure and Properties of Water*; Oxford University: New York, 1969.

(28) Norby, P. ; Norlund, C. A. *Acta Chem. Scand.* **1986**, *A40*, 500.

(29) Rudolf, P. R.; Crowder, C. E. *Zeolites* **1990**, *10*, 163. McCusker, L. B.; Baerlocher, C.; Jahn, E.; Bulow, M. *Zeolites* **1991**, *11*, 308. Prasad, S.; Vetrivel, R. *J. Phys. Chem.* **1994**, *98*, 1579.

(30) Taylor, R.; Kennard, O. *Acc. Chem. Res* **1984**, *17*, 320.

(31) Jeffrey, G. A.; Lewis, L. *Carbohydrate Res.* **1978**, *60*, 179.

(32) Bell, R. P.; *Proc. R. Soc. London* **1936**, *A154*, 414. Evans, M. G.; Polanyi, M. *Trans. Faraday Soc.* **1938**, *34*, 11. Dewar, M. J. S. *The Molecular Orbital Theory of Organic Chemistry*; McGraw-Hill: New York, 1969.